Estimation of subsurface soil moisture from surface soil moisture in cold mountainous areas

Jie Tian[1,2], Zhibo Han[1], Heye Reemt Bogena[2], Johan Alexander Huisman[2], Carsten Montzka[2], Baoqing Zhang[1*], Chansheng He[1,3*]

[1]Key Laboratory of Western China's Environmental Systems (Ministry of Education), College of Earth and Environmental Sciences, Lanzhou University, Lanzhou, Gansu 730000, China

[2]Agrosphere Institute (IBG-3), Forschungszentrum Jülich, 52425 Jülich, Germany

[3]Department of Geography, Western Michigan University, Kalamazoo, MI 49008, USA

Correspondence to: Baoqing Zhang (baoqzhang@lzu.edu.cn) and Chansheng He (he@wmich.edu)

Abstract. Profile soil moisture (SM) in mountainous areas is important for water resources management and ecohydrological studies of downstream arid watersheds. Satellite products are useful in providing spatially distributed SM information, but only have limited penetration depth (e.g. top 5 cm). In contrast, in situ observations can provide multi-depth measurements, but only with limited spatial coverage. Spatially continuous estimates of subsurface SM can be obtained from surface observations using multiple methods. This study evaluates methods to calculate subsurface SM from surface SM and its application to satellite SM products based on a SM observation network in the Qilian Mountains (China) established since 2013. First, three different methods were tested to estimate subsurface (10-20, 20-30, 30-50, 50-70 cm, and profile of 0-70 cm) SM from in-situ surface SM (0-10 cm): the exponential filter (ExpF), the artificial neural network (ANN) and the cumulative distribution function matching (CDF) methods. The results showed that both ANN and ExpF methods were able to provide accurate estimates of subsurface soil moisture at 10-20 cm, 20-30 cm, and for the profile of 0-70 cm using surface (0-10 cm) soil moisture only. Specifically, the ANN method had the lowest estimation errors (RSR) of 0.42, 0.62 and 0.49 for depths of 10-20 and 20-30 cm and profile SM, respectively, while the ExpF method best captured the temporal variation of subsurface soil moisture. Furthermore, it was shown that the performance of profile SM estimation was not significantly worse when an area-generalized T_{opt} (optimum T) was used instead of station-specific T_{opt} for the Qilian Mountains. In a final step, the ExpF method was applied to obtain profile soil moisture from the SMAP_L3 surface soil moisture product, and the resulting profile SM was compared with in situ observations. The results showed that the ExpF method was able to estimate profile SM from SMAP_L3 surface data with reasonable accuracy (median R of 0.65). It was also found that the combination of ExpF method and SMAP_L3 surface product can significantly improve the estimation of profile SM in mountainous areas compared to the SMAP_L4 root zone product. Overall, it was concluded that the ExpF method is useful and has potential for estimating profile SM from SMAP surface products in the Qilian Mountains.

1. Introduction

Soil moisture (SM) is considered to be an essential climate variable (Bojinski et al., 2014) because of its critical role in the water, energy (Jung et al., 2010) and carbon cycle (Green et al., 2019). In particular, knowledge of profile SM is important for runoff modeling (Brocca et al., 2010), water resources management (Gao et al., 2018), drought assessment (Jakobi et al., 2018), and climate analysis (Seneviratne et al., 2010). Methods for SM measurements include ground-based measurements and satellite-based methods (Dobriyal et al., 2012). Most ground-based methods enable the determination of SM changes with high temporal resolution at different depths, but with limited spatial coverage (Jonard et al., 2018). Especially in mountainous regions, in situ SM measurements at large scales are difficult to obtain and thus scarce (Ochsner et al., 2013). In addition, strong SM heterogeneity in complex mountainous areas makes SM estimation at large scales more difficult (Williams et al., 2009). By comparison, satellite estimates of SM, such as those from the Soil Moisture Active & Passive (SMAP) mission, provides spatial SM coverage at large scale (Entekhabi et al., 2014; Brocca et al., 2017). Unfortunately, SMAP and other microwave-based SM products from spaceborne sensors only provide SM estimates for a limited depth up to ~5 cm (Escorihuela et al., 2010). Thus, a gap exists with respect to the availability of deeper SM information with adequate spatial coverage.

Previous studies have shown that subsurface SM is often related to surface-near SM (Mahmood and Hubbard, 2007; Wang et al., 2017). A variety of approaches for estimating deep SM from surface SM information has been developed, including data assimilation of remote sensing data into land surface models (Han et al., 2013), physically-based methods (Manfreda et al., 2014), (semi-) empirical approaches (Albergel et al., 2008), data-driven methods (Kornelsen and Coulibaly, 2014; Zhang et al., 2017a), and statistical methods (Gao et al., 2019). Among them, the application of both data assimilation and physically based methods are limited to data-rich areas due to the large amount of required input data, e.g. soil properties, which are often not available for data-scarce mountainous areas (Jin et al., 2015; Li et al., 2017; Dai et al., 2019). The Cumulative Distribution Function (CDF) matching approach is a statistical method developed to adjust systematic differences in different SM datasets (e.g. in-situ observations and satellite products) based on observation operators (Drusch et al., 2005; Peng et al., 2017). CDF matching can also be used for upscaling of SM (Han et al., 2012) and estimating subsurface SM from surface SM (Gao et al., 2019). Artificial neural network (ANN) is effective and powerful data-driven tools for nonlinear estimation problems, and has been widely used to estimate subsurface SM from surface SM measurements (Kornelsen and Coulibaly, 2014; Pan et al., 2017). The exponential filter (ExpF) method belongs to the semi-empirical modeling approaches and relies on a two-layer SM balance equation (Wagner et al., 1999). This method has been widely applied with both in situ observations and satellite products, and the performance of the ExpF method for estimating subsurface SM varied considerably over regions with different environmental conditions (Ford et al., 2014; González-Zamora et al., 2016; Tobin et al., 2017; Wang et al., 2017; Zhang et al., 2017a). Ford et al. (2014) found that root zone SM estimated from SMOS satellite products had a mean R^2 of 0.57 (ranging from 0.00 to 0.86) and 0.24 (ranging from 0.00 to 0.51) for SM networks in Oklahoma and Nebraska, respectively. In addition to surface SM data, the ExpF method requires only one additional parameter (T, the characteristic time) that reflects the joined

influence of local conditions on the temporal characteristics of SM (Albergel et al., 2008; Ceballos et al., 2005). Previous studies have shown that T varied among different stations and several methods have been developed to estimate T (Wagner et al., 1999; Albergel et al., 2008; Brocca et al., 2010; Qiu et al., 2014).

Methods for estimating deeper SM from surface SM have not been evaluated for high and cold mountainous areas using large scale in-situ SM observations. In the absence of large-scale in-situ SM observation networks, satellite SM products can be an alternative for providing large scale surface SM information (Ochsner, et al., 2013). Although SM estimation from spaceborne sensors is especially challenging for mountainous regions, some validation activities have shown adequate accuracy (Pasolli et a., 2011; Rasmy et al., 2011; Zhao et al., 2014; Zeng et al., 2015; Zhao and Li, 2015; Colliander et al., 2017; Ullah et al., 2018; Qu et al., 2019; Liu et al., 2019). Nevertheless, the accuracy of profile SM estimation from remotely sensed SM products is currently unknown for mountainous regions.

In this study, we focus on the Qilian Mountains, which is a water source for several key inland rivers with terminal lakes in Northwest China, including the Heihe, Shiyang, and Shule Rivers (He et al., 2018). Water scarcity threatens both food and ecosystem security in these endorheic basins (Feng et al., 2019). At the northeastern border of the Tibet-Qinghai plateau with its significant role in the Asian monsoon, profile water content in the Qilian Mountains is a key variable in ecohydrological studies on water resources and exchange processes in these basins (Zhao et al., 2013). Therefore, the aim of this study is to use multi-station in situ SM observations and remotely sensed SM data from the Qilian Mountains, a prime example of a high and cold mountainous area, to characterize the relationship between surface SM and deeper SM in order to obtain the spatial distribution of profile SM. We first evaluated the performance of the different methods for estimating subsurface SM. Subsequently, the best method was employed with SMAP surface SM products to evaluate its utility for estimating profile SM in mountainous regions.

2. Study Area

This study was carried out in the upland area of the Heihe River Basin, which is a typical terminal lake basin of the arid regions (Liu et al., 2018) (Fig 1). It is located in the Qilian Mountains at the Northeastern border of the Qinghai-Tibet plateau. It covers approximately 2.7×10^4 km^2 and the elevation ranges from about 2000 to 5000 m (Yao et al., 2017). The region has an annual precipitation ranging from 200 to 500 mm (Luo et al., 2016), annual potential evapotranspiration ranging from 700 to 2000 mm, and an annual mean temperature ranging from -3.1 °C to 3.6 °C during 1960-2012 (He et al, 2018). The main land covers are grassland, forestland and sparsely vegetated land (Zhou et al., 2016). The main soil types are Calcic Chernozems, Kastanozems, and Gelic Regosols. The main soil texture classes are silt loam, silt and sandy loam (Tian et al., 2017; 2019).

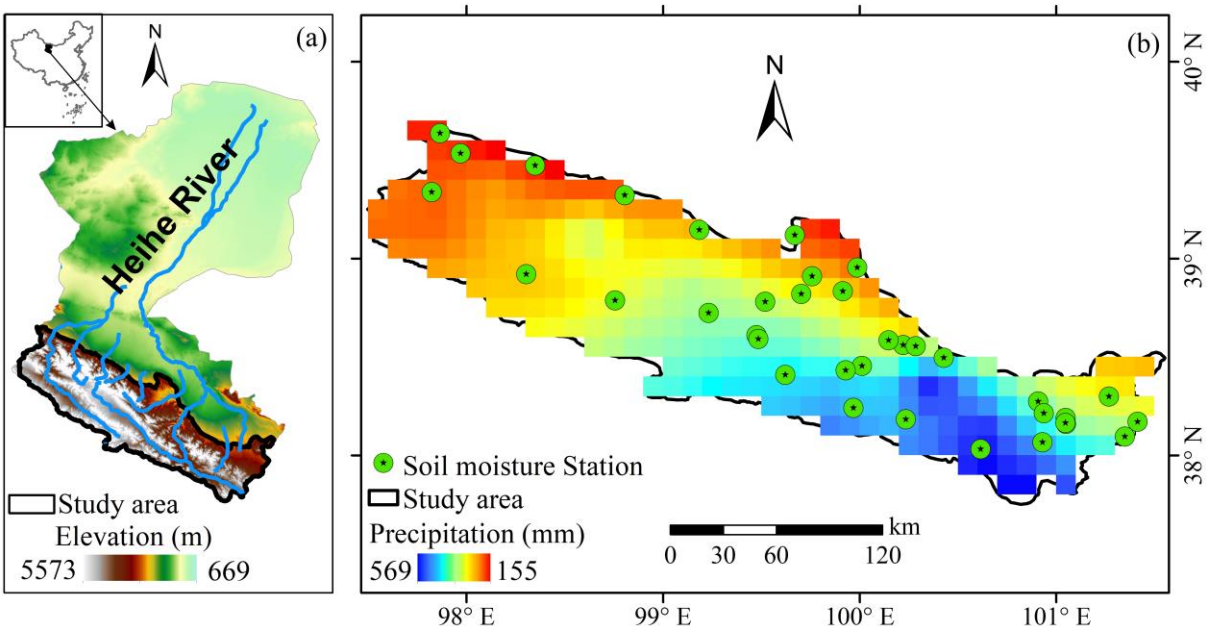

Fig. 1. (a) Study area and **(b)** distribution of the SM stations with spatial distribution of annual average precipitation from 2014 to 2016.

3. Data and Methods

3.1. Datasets

A SM monitoring network was set up in September 2013 in the Qilian Mountains. The network is composed of 35 SM stations distributed over the entire study area (Fig. 1). At each station, SM profiles from 0 to 70 cm were measured by soil moisture probes (ECH2O 5TE, METER Group Inc., USA) installed at depths of 5 (representing depth of 0-10 cm, $SM_{5\ cm}$), 15 (10-20 cm, $SM_{15\ cm}$), 25 (20-30 cm, $SM_{25\ cm}$), 40 (30-50 cm, $SM_{40\ cm}$) and 60 cm (50-70 cm, $SM_{60\ cm}$) below the soil surface at 30 min intervals. Soil-specific sensor calibrations were performed with the direct calibration method using soil samples taken from each station (Cobos and Chambers, 2010; Zhang et al., 2017b). The profile integrated SM ($SM_{0\text{-}70\ cm}$) was calculated by the method of González-Zamora et al. (2016):

$$SM_{0-70\ cm} = \frac{SM_{5\ cm}\times 10 + SM_{15\ cm}\times 10 + SM_{25\ cm}\times 10 + SM_{40\ cm}\times 20 + SM_{60\ cm}\times 20}{70} \quad (1)$$

The entire data set used in this study thus consists of six in situ SM time series at depths of 5, 15, 25, 40, 60 cm, and 0-70 cm for each of the 35 stations. Due to the influence of soil freezing in winter, the soil moisture time series were limited to the growing seasons (May to October, Tian et al., 2019) of 2014, 2015 and 2016. The half-hourly measurements were averaged to obtain daily SM values for the estimation of subsurface SM (Wagner et al., 1999). Data quality management was performed for each station, and data gaps existed in the harsh mountainous environment, as described in detail in Tian et al. (2019). Time series where the amount of missing values exceeded 50% were excluded in the analysis. The final dataset after processing is

presented in Fig. 2. The surface SM measured at 5 cm was used to predict the subsurface SM at depths of 15, 25, 40, 60 cm and the profile average (0-70 cm).

Soil cores were taken to measure soil properties including soil organic carbon (SOC), saturated hydraulic conductivity (K_S), soil particle composition and bulk density for each layer during the sensor installation. Detailed descriptions of the soil properties can be found in Tian et al. (2017; 2019). The statistics of the soil physical characteristics are provided in Table 1. Daily precipitation from reanalysis (Chen et al., 2011), Landsat-based continuous monthly 30m×30m resolution NDVI data for the period 1986-2017 (Cihlar et al., 1994; Huete et al., 2002; Wu et al., 2019) were acquired from the National Tibetan Plateau Data Centre (https://data.tpdc.ac.cn/en/).

The widely used higher level SMAP_L3 Global Daily 9 km product for the growing seasons of 2015 to 2017 were used in this study (O'Neill et al., 2018). This product is distributed by NASA (http://nsidc.org/). SMAP descending node observations acquired near 6:00 AM local solar time have been combined to global daily composites in order to reduce the impact of Faraday rotation and to consider the assumption of uniform temperature profiles in the vegetation cover during morning overpasses. It has to be noted that the data are provided on a 9 km grid, but that this is a result of a Backus-Gilbert optimal interpolation at brightness temperature level. The actual spatial resolution is coarser (O'Neill et al., 2018). SMAP_L3 surface soil moisture product was also used to estimate the subsurface soil moisture (Layer 2: 10-20 cm, Layer 3: 20-30 cm, Layer 4: 30-50 cm, Layer 5: 50-70 cm) and profile soil moisture (0-70 cm) during the growing seasons of 2015 and 2016 in the mountainous area.

SMAP_L4 provides estimates of both surface and root zone SM products based on the assimilation of brightness temperature into the NASA land-surface model, and it has a spatial and temporal resolution of 9 km and 3 h, respectively, (Reichle et al., 2017). SMAP_L4 is a widely used root zone SM product (Pablos et al., 2018). Here, the SMAP_L4 data were averaged to a daily resolution in order to compare it with the profile SM estimates from the SMAP_L3 surface product obtained in this study. In particular, the SMAP_L4 SM product with both surface (0-5 cm, sm_{0-5}) and root zone (0-100 cm, sm_{0-100}) information were used to calculate SM of the 0-70 cm profile (sm_{0-70}) using:

$$sm_{0-100} = (5 * sm_{0-5} + 95 * sm_{5-100})/100 \quad (2)$$

$$sm_{0-70} = (5 * sm_{0-5} + 65 * sm_{5-100})/70 \quad (3)$$

Table 1. Statistics of the soil physical characteristics at the 35 soil moisture stations: mean (standard deviation)

Layer	Depth (cm)	Bulk Density (g/cm^3)	K_S (cm/hour)	SOC (g/100g)	Sand (%)	Silt (%)	Clay (%)
Layer 1	0-10	1.13(0.28)	3.87(4.11)	4.35(4.11)	26.6(11.9)	66.2(10.9)	7.2(1.6)
Layer 2	10-20	1.14(0.24)	4.61(4.53)	3.9(3.87)	24.5(11.9)	68.6(11.2)	6.9(1.2)
Layer 3	20-30	1.18(0.32)	4.78(6.22)	3.63(3.54)	27.0(15.2)	66.5(14.3)	6.5(1.4)
Layer 4	30-50	1.29(0.3)	3.94(4.68)	2.21(2.28)	29.5(15.3)	63.8(14.5)	6.5(1.6)
Layer 5	50-70	1.34(0.3)	1.85(2.35)	2.34(2.47)	26.9(17.1)	66.5(15.9)	6.7(1.9)

Note: K_S is the Saturated Hydraulic Conductivity; SOC is the Soil Organic Carbon.

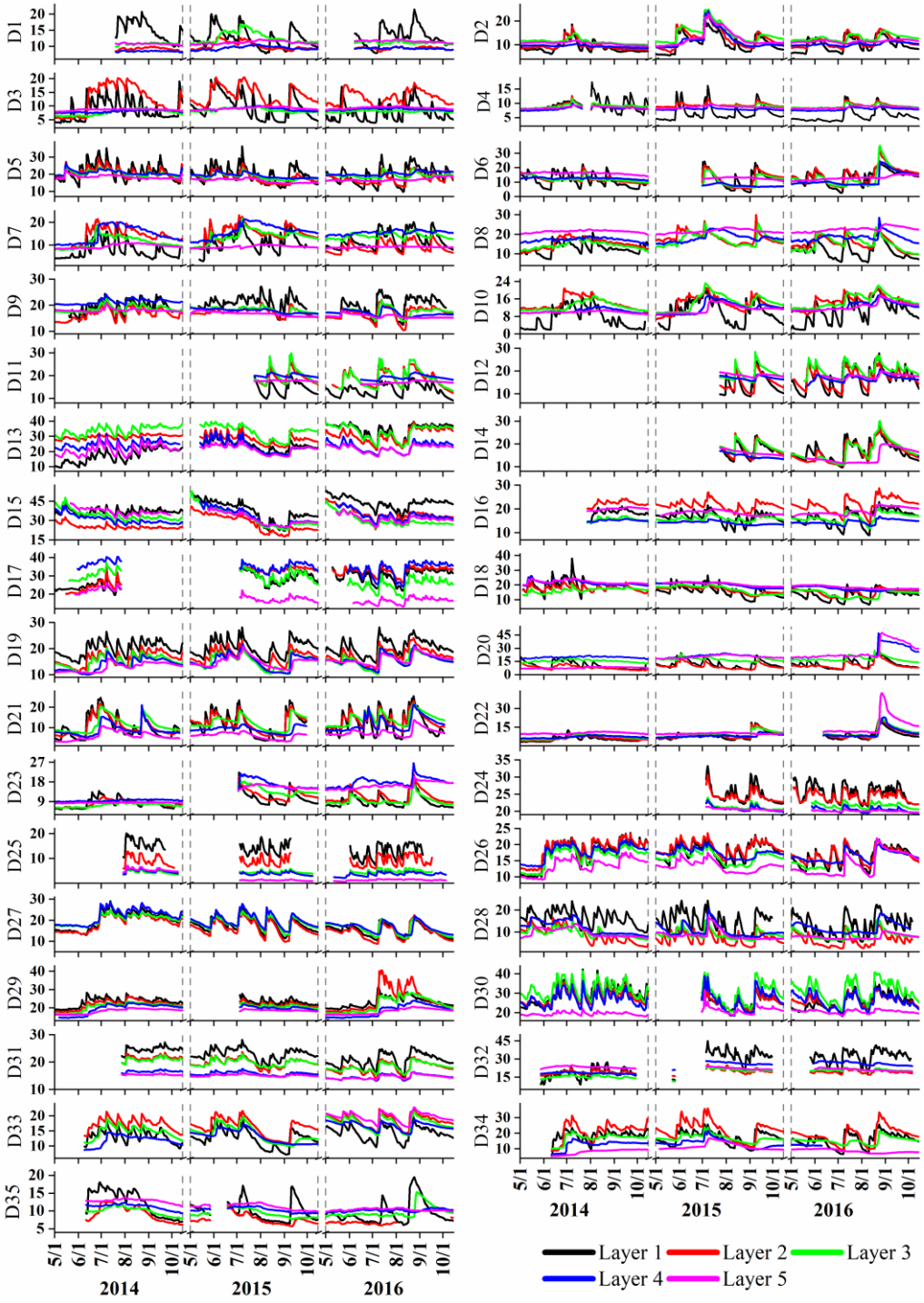

135

Fig. 2. Daily soil moisture (vol. %) time series during the growing season of 2014 to 2016 for the 5 layers (layer 1, 0-10 cm; layer 2, 10-20 cm; layer 3, 20-30 cm; layer 4, 30-50 cm; layer 5, 50-70 cm) in the 35 soil moisture stations. Gaps exist for some stations due to missing data.

3.2. Exponential Filter (ExpF) method

The ExpF method predicts the dynamics of subsurface SM using an exponential filter function of the surface SM dynamics (Wagner et al., 1999; Albergel et al., 2008). First, SM (cm^3/cm^3) is transformed into a soil water index (SWI) with:

$$SWI_i = \frac{\theta_i - \theta_{i,min}}{\theta_{i,max} - \theta_{i,min}} \quad (4)$$

where $\theta_{i,min}$ and $\theta_{i,max}$ are the minimum and maximum SM in the time series collected since installation for each layer of each station (Ford et al., 2014). The ExpF method then estimates subsurface SM from surface SM using:

$$SWI_{m,t_n} = SWI_{m,t_{n-1}} + K_{t_n}(ms_{t_n} - SWI_{m,t_{n-1}}) \quad (5)$$

where $SWI_{m,t_{n-1}}$ and SWI_{m,t_n} are the predicted subsurface SWI at time t_{n-1} and t_n, respectively. ms_{t_n} is the observed surface SWI at time t_n, and K_{t_n} represents the gain at time t_n calculated by:

$$K_{t_n} = \frac{K_{t_{n-1}}}{K_{t_{n-1}} + e^{-\frac{t_n - t_{n-1}}{T}}} \quad (6)$$

where $K_{t_{n-1}}$ is the gain at time t_{n-1} and T is the characteristic time length in days. The equation was initialized with $SWI_{m,t_1} = ms_{t_1}$ and $K_{t_1} = 1$ (Albergel et al., 2008). This method is particularly useful as T is the only unknown parameter. The optimum T (T_{opt}) was determined by optimization using the highest Nash-Sutcliffe score for each specific depth at each station.

3.3. Artificial Neural Network (ANN) method

The ANN method is a data-driven method to predict subsurface SM from surface SM (Zhang et al., 2017a). If properly trained, ANN are able to describe nonlinear relationships between dynamics of SM at different depths (Kornelsen and Coulibaly, 2014). The commonly used feed-forward ANN (with one hidden layer and 10 neurons, Levenberg–Marquardt algorithm, Ford et al., 2014) was used in this study and the ANN modelling was carried out using MATLAB (neural network time series tool, R2017b, The MathWorks). The output of the ANN was calculated using:

$$y = f[W_2 g(W_1 X + b_1) + b_2] \quad (7)$$

where y is the output, f and g are the activation functions of the hidden layer and the input layer, respectively, W_1 and W_2 are the weights of the input layer and the hidden layer, respectively, and $b1$ and $b2$ are the biases of the input layer and the hidden layer, respectively. The tangent sigmoid function was used as the activation function as it has shown good performance in hydrological studies (Yonaba et al., 2010). As suggested by Zhang et al. (2017a), 70% of data were randomly selected for training the ANN and the remaining 30% were used for validation. A separate ANN model was developed for every depth combination and every site.

3.4. Cumulative Distribution Function matching (CDF) method

In this study, the following procedure for CDF matching was used:

1) Rank the surface (θ_1) and the subsurface SM (θ_2) time series;

2) Calculate the difference between the two observation time series:

$$\Delta_i = \theta_{1,i} - \theta_{2,i} \quad (8)$$

3) Use a cubic polynomial fit to relate the difference (Δ) to surface SM (θ_1) as recommended by Gao et al. (2019):

$$\hat{\Delta} = K_0 + K_1 \cdot \theta_1 + K_2 \cdot {\theta_1}^2 + K_3 \cdot {\theta_1}^3 \quad (9)$$

where $\hat{\Delta}$ is the predicted difference between surface and subsurface SM, and K_i (i=0,1,2,3) are parameters.

4) Calculate CDF-matched subsurface SM (θ_{CDF}) with:

$$\theta_{CDF} = \theta_1 - \hat{\Delta} \quad (10)$$

Similar to the ANN method, 70% of the data were used to calibrate the approach and the remaining 30% of the data were used for validation of the CDF matching method.

3.5. Statistical analysis

Boxplots were used to show the scatter of the data. The difference between data in different groups was examined using a one-way analysis of variance (ANOVA) with the post-hoc Bonferroni test when the normality and homogeneity of variance of the datasets were satisfied. The Kruskal-Wallis ANOVA with a post-hoc Dunn's test was used in case these conditions were not satisfied (Lange et al., 2008). The statistical analysis was performed in SPSS (SPSS 18.0, SPSS Inc.) and Matlab (R2017b, The MathWorks). The significance level was 0.05 for all statistical tests.

4. Results and discussion

4.1. Evaluation of different methods

The ExpF method estimates subsurface SM based on SWI, while the ANN and CDF methods are based on volumetric soil moisture. Following Moriasi et al. (2007), the Nash-Sutcliffe efficiency (NSE), the ratio of RMSE to the standard deviation of the observations (RSR, an error statistic that normalizes the RMSE), and Pearson correlation coefficient (R) were used to evaluate the performance of different methods with different units. Fig. 3, Table 2 and Fig. S1 summarize the metrics (NSE, RSR, and R) for subsurface SM estimates at different depths obtained using different methods for the growing season of 2014, 2015 and 2016. Fig. 3 shows that there were significant differences for the NSE of different methods for all layers ($p<0.05$). The ANN had the highest NSE with a median value of 0.82, 0.56, 0.35, 0.35 and 0.76 for layers 2, 3, 4, 5 and profile SM, respectively. There were no significant differences between the ExpF and the CDF matching method for layer 2, layer 3 and

the profile SM. The CDF matching method showed the lowest NSE for layers 4 and 5. Overall, both the ANN and ExpF methods showed good performance in terms of NSE for layer 2, layer 3 and profile SM (median NSE > 0.5), and the CDF matching method showed a good performance in terms of NSE for layer 2 and profile SM (median NSE > 0.5).

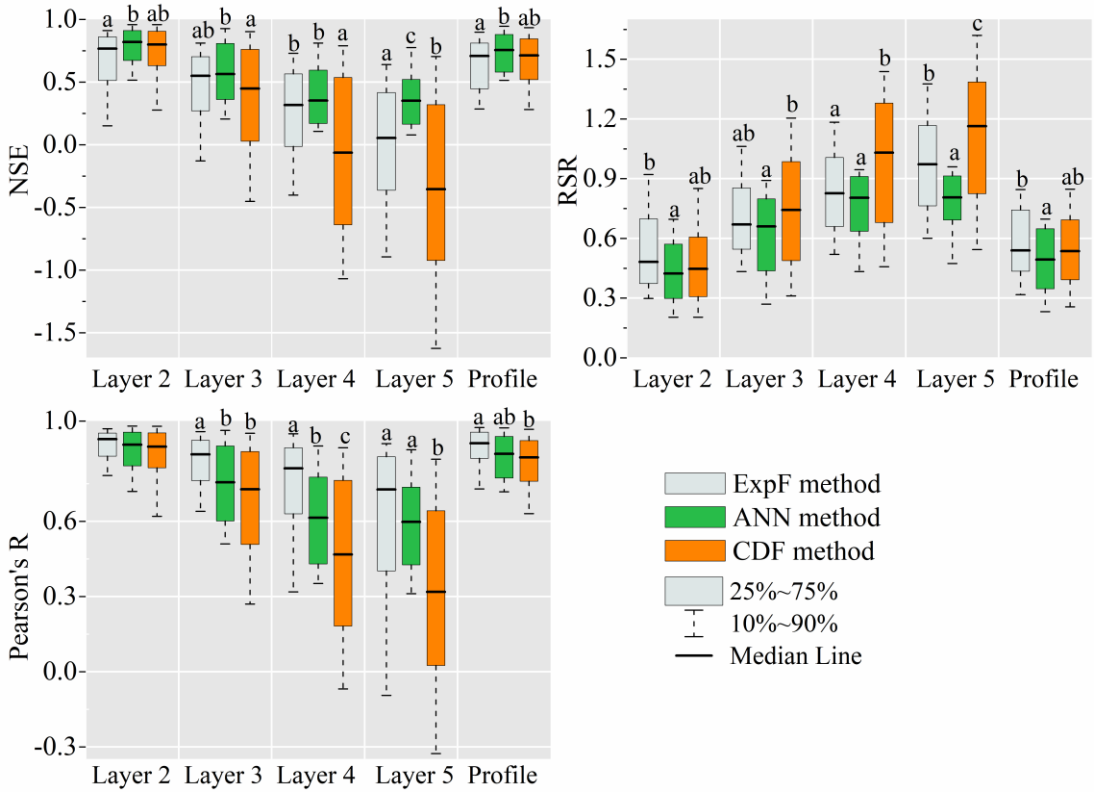

Fig. 3. Boxplot of the metrics (NSE, RSR, R) to compare the subsurface SM estimation using surface SM through the three methods (ExpF, ANN, CDF) with the observations for the 35 stations during the growing seasons of 2014 to 2016. Different letters above the box indicate the significant difference ($p<0.05$) among different methods.

Similar to the results for NSE, Fig. 3 shows that the ANN method resulted in a significantly lower RSR ($p<0.01$) for all depths. There were no significant differences between the ExpF and CDF matching method for layer 2, layer 3 and profile SM, and the CDF matching method showed a significantly higher RSR for layer 4 and layer 5. The ExpF method had a similar estimation error as the CDF matching method for layer 2, layer 3 and profile SM. Both the ANN and ExpF methods showed satisfactory results (RSR<0.7) for layer 2, layer 3 and profile SM, and the CDF matching method showed satisfactory results for layer 2 and profile SM (Moriasi et al., 2007).

Fig. 3 shows that the ExpF method resulted in the highest R for all layers (with a median value of 0.93, 0.87, 0.81, 0.73 and 0.91 for layers 2, 3, 4, 5 and profile SM, respectively), while the CDF matching method resulted in the lowest R for all layers (with a median value of 0.90, 0.73, 0.47, 0.32 and 0.86 for layers 2, 3, 4, 5 and profile SM, respectively). The good performance for R suggests that the ExpF method had the best ability to describe the temporal variability in SM.

Table 2. The statistics (mean±standard deviation) of the performance (RSR, R and NSE) of different methods (ExpF, ANN, and CDF) for estimating subsurface SM using surface SM for each layer of 35 stations during the growing seasons of 2014, 2015, and 2016

Layer	RSR			R			NSE		
	ExpF	ANN	CDF	ExpF	ANN	CDF	ExpF	ANN	CDF
Layer 2	0.55±0.25	0.44±0.20	0.50±0.27	0.89±0.10	0.87±0.13	0.84±0.19	0.63±0.36	0.76±0.21	0.68±0.37
Layer 3	0.72±0.27	0.62±0.23	0.75±0.34	0.81±0.19	0.74±0.18	0.66±0.29	0.41±0.50	0.56±0.28	0.33±0.56
Layer 4	0.83±0.27	0.75±0.22	0.99±0.37	0.70±0.31	0.61±0.21	0.44±0.37	0.24±0.47	0.40±0.29	-0.11±0.71
Layer 5	0.97±0.29	0.77±0.19	1.11±0.38	0.57±0.39	0.58±0.22	0.3±0.41	-0.03±0.61	0.37±0.26	-0.38±0.82
Profile	0.58±0.22	0.49±0.19	0.54±0.22	0.88±0.11	0.85±0.11	0.83±0.13	0.61±0.32	0.73±0.18	0.66±0.26

As expected, all metrics showed that the performance decreased with depth. The results indicate that for two out of the three statistical measures (i.e. RSR and NSE), the ANN method was statistically superior to the other two methods. Results also demonstrated that both ANN and ExpF method were able to provide accurate estimates of subsurface SM for layer 2, layer 3 and profile SM. Specifically, the ANN method resulted in the lowest estimation error, while the ExpF method was better able to capture SM dynamics. A similar finding was reported by Zhang et al. (2017a), who found that the ExpF method had a significantly higher correlation coefficient along with a higher mean bias compared to the ANN method. Furthermore, the ExpF method is a simpler approach as it only needs one parameter (T_{opt}), and can thus be easily applied in data-scarce mountainous areas, while the establishment of the ANN method is much more complicated. Besides, the ExpF method is a process-based method, while ANN is the machine learning method. Therefore, the ExpF method was used to estimate subsurface SM in the remainder of this study.

4.2. Evaluation of T_{opt} for the ExpF method

4.2.1. Variation of T_{opt} with depth

It was found that the accuracy of the ExpF method varied with the selected T value, and that higher T values resulted in more stable estimation of SM time series (Wagner et al., 1999; Albergel et al., 2008). Furthermore, it was found that each station had an optimum T (T_{opt}) as determined based on the best match with observations in terms of NSE. The variation of NSE with T (ranging from 0 to 68 days) for different layers for each station is shown in Fig. 4 and Table 3. It can be seen that the sensitivity of high values of NSE to changes in T decreased with increasing depth, indicating that the range of T values with high NSE was larger deeper in the soil. This was also observed in previous studies (e.g. Wang et al., 2017).

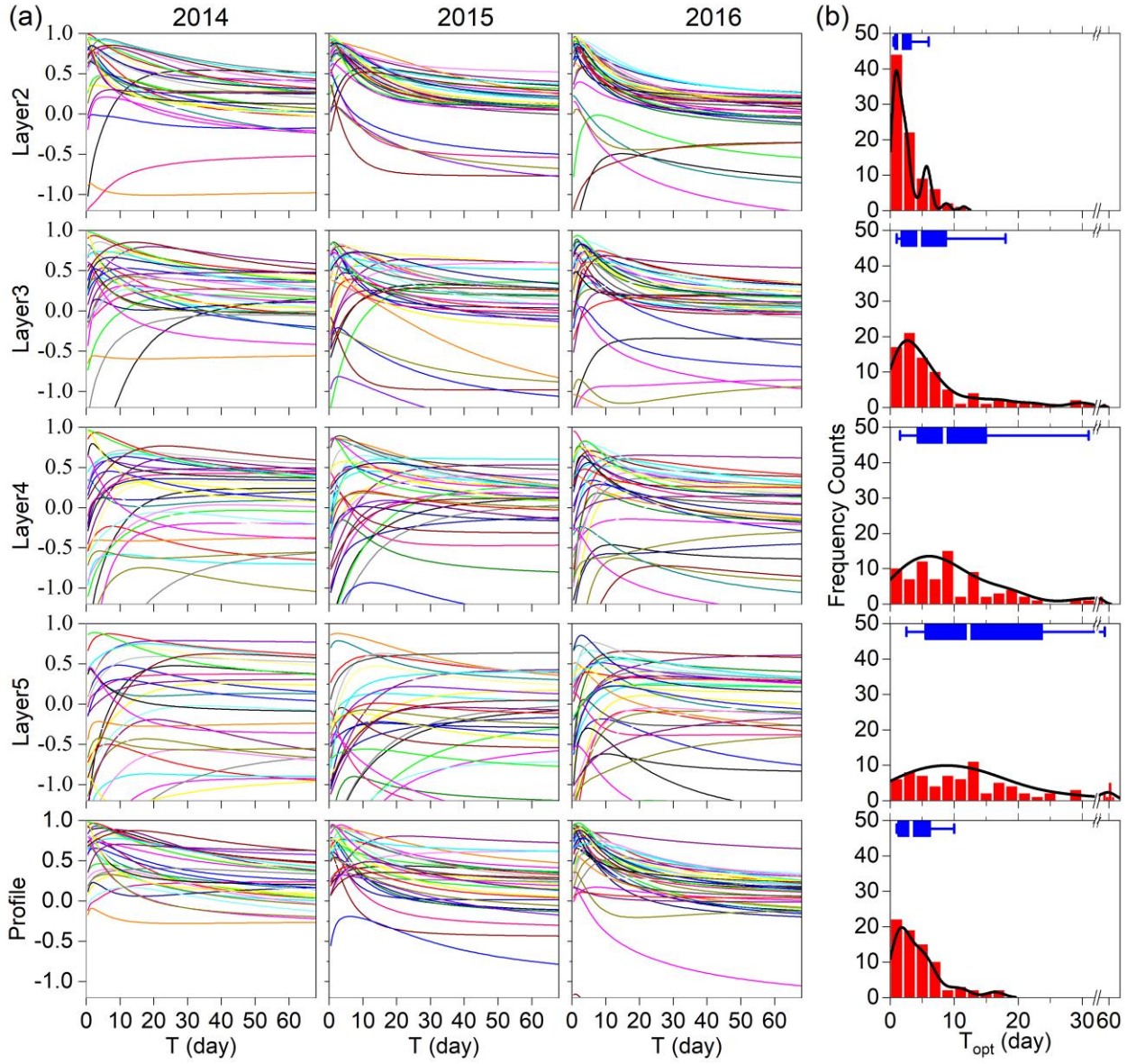

Fig. 4. Variation of NSE with T of the exponential filter method at different layers of each stations during the growing season of 2014, 2015 and 2016. Y axis is the NSE value. Frequency distribution curve and histogram to show the distribution of T_{opt} with depth for all stations.

Results of a two-way ANOVA showed that the difference of T_{opt} is not significant between different years ($p=0.06$) while differences were significant between layers ($p<0.001$). Furthermore, it can be seen that T_{opt} increased with depth from layer 2 to 5. The median of T_{opt} ranged from 1.5 for layer 2 to 12.5 days for layer 5. The median T_{opt} for profile SM was 3.5 days. Significant differences in T_{opt} were obtained for layer 2, layer 3, and layer 4, but the difference between layers 4 and 5 was not significant. The increase of T_{opt} with depth has already been observed in many studies, and is related to the greater temporal stability of SM in deeper soil layers (Wang et al., 2017; Tian et al., 2019).

Table 3. The statistics of T_{opt} (day) for different layers and different years for all stations.

Year	Statistics	Layer 2	Layer 3	Layer 4	Layer 5	Profile
2014	mean (std)	2.72 (2.22)	8.32 (8.39)	13.18 (12.52)	16.81 (16.70)	4.73 (4.16)
	median	2.00	5.50	9.50	12.75	4.00
2015	mean (std)	2.56 (2.54)	7.78 (8.04)	15.77 (15.87)	23.15 (19.61)	5.23 (4.51)
	median	1.50	5.00	9.00	12.00	3.75
2016	mean (std)	2.23 (2.13)	6.13 (9.80)	9.26 (9.43)	17.74 (18.93)	3.32 (2.56)
	median	1.50	4.00	6.50	12.50	2.75
Summary	mean (std)	2.48(2.26)[a]	7.29(8.85)[b]	12.37(12.67)[c]	18.93(18.43)[c]	4.32(3.77)[ab]
	median	1.50	4.50	8.50	12.50	3.50

Note: std represents the standard deviation. Summary represents the statistics results of the three years. Different letters in Summary row indicate significant differences among different layers ($p<0.05$), while the same letter indicates that the difference is nonsignificant.

4.2.2 Evaluation of alternative methods for T_{opt} estimation

Previous studies have used various methods to estimate T_{opt}. For example, it was found that using a single representative value for T_{opt} (e.g. average or median) for all stations did not significantly reduce the accuracy of the SM estimates (Albergel et al., 2008; Ford et al., 2014). Wagner et al. (1999) recommended a common value of $T_{opt} = 20$ (days) to estimate root zone SM, and this value has been widely adopted (e.g. Lange et al., 2008; Muhammad et al., 2017). Qiu et al. (2014) proposed to estimate T_{opt} using the station-specific long-term mean NDVI using $T_{\mathrm{opt}} = -75.263 \times \mathrm{NDVI} + 68.171$ (R=0.5, $p<0.01$). This approach has also been applied in other studies (Tobin et al., 2017).

Here, we evaluated four different methods to estimate T_{opt} in our study region for estimating profile soil moisture (0-70 cm, SWI) from surface soil moisture (5 cm, SWI). In the first method, T_{opt} was estimated from the NDVI-based regression of Qiu et al. (2014) to provide T_{Qiu}. In the second method, T_{opt} was set to 20 days as recommended by Wagner et al. (1999) to provide T_{Wagner}. In the third method, an area-generalized T_{opt} was obtained from the median value for the profile SM in our study region (3.5 days) to provide $T_{general}$. In the fourth and final method, the original station-specific T_{opt} parameter for profile SM was used ($T_{specific}$). The accuracy of the SM estimates obtained using the different methods to estimate T_{opt} was again evaluated using NSE, R and RMSE (Fig. 5). The performance metrics show that $T_{specific}$ performed best (mean RSR of 0.58, R of 0.88, and NSE of 0.61) followed by $T_{general}$ (mean RSR of 0.61, R of 0.85, and NSE of 0.58), T_{Wagner} (mean RSR of 0.79, R of 0.69, and NSE of 0.32) and T_{Qiu} (mean RSR of 0.89, R of 0.59, and NSE of 0.17). However, the difference in performance between $T_{specific}$ and $T_{general}$ is not significantly different. The T_{Wagner} and the T_{Qiu} approach performed less well, and the metrics (NSE, R, RSR) are significantly ($p<0.001$) lower than those of the $T_{general}$ and $T_{specific}$ methods. Our results suggest that a site-specific T_{opt} significantly improves the performance of the ExpF method compared to the use of the universal T_{opt} recommended by Wagner et al. (1999) or the regression of Qiu et al. (2014). Similarly, Lange et al. (2008) also found a significant improvement when using a station-specific T_{opt} instead of $T_{opt} = 20$ days. It should be mentioned that the estimation depth in the method of Wagner et al. (1999) was 0-100 cm, while that of our study was 0 - 70 cm. This may partly explain the poor performance of

the T_{Wagner} approach in this study. The use of an area-generalized T_{opt} (3.5 days) is a suitable alternative for T_{opt} estimation in our study area, and provides similar estimation performance. Other studies have also found a good performance when using an area-generalized T_{opt} (e.g. Albergel et al., 2008; Brocca et al., 2010; Ford et al., 2014).

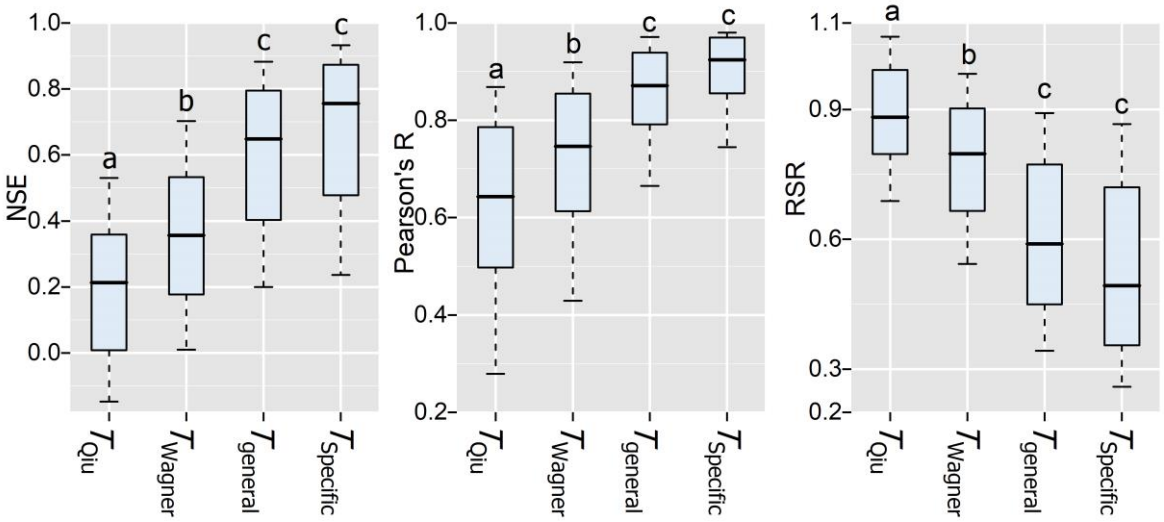

Fig. 5. The boxplot of NSE, Pearson's R, and RSR for the T_{opt} generated from different schemes. The different letters above box indicate the significant difference for different schemes.

4.3 Estimating profile soil moisture using SMAP

The results have shown that the ExpF method is suitable to estimate profile SM from surface SM. Moreover, the evaluation of methods for T_{opt} estimation concluded that the median value of T_{opt} is suitable for estimation of subsurface soil moisture. Thus, in this section, we evaluate the utility of the ExpF method (with the median value of T_{opt} of SMAP) in combination with SMAP surface products for estimating subsurface SM in mountainous areas.

4.3.1 Assessment of SMAP surface SM product

The observed surface SM of each station was compared with the SMAP_L3 soil moisture product that overlapped with the corresponding station for the growing seasons of 2015 and 2016 for all stations to evaluate the accuracy of the SMAP measurements (Pablos et al., 2018). The root mean square error (RMSE), mean bias error (MBE), unbiased RMSE (ubRMSE) and R were adopted as metrics to evaluate accuracy. The relationship between the SMAP_L3 SM data product and the in-situ observations a 5 cm depth is presented in Fig.6. Clearly, the part of the scatter in the relationship is due to the scale discrepancy between the satellite and the in-situ SM sensor data. Nevertheless, the statistical metrics still indicate a significant relationship between the SMAP_L3 SM data product and the in-situ observations a 5 cm depth. Time series of the two datasets for each station are provided in the supplementary Fig. S2. Figs. 6 and S2 show that the performance was low at two stations (D13 with R of 0.18, D15 with R of 0.08) with scrubland and relatively high soil moisture. The poor performance at scrubland sites is consistent with results presented by Zhang et al. (2017b) for this study region. Results showed that the MBE varied from -0.23

to 0.07 cm^3/cm^3 with a median of -0.021 cm^3/cm^3. This indicates that SMAP underestimated surface SM over the study region, which is consistent with previous studies in the area (Chen et al., 2017; Zhang et al., 2017b). The RMSE varied between 0.026 and 0.250 cm^3/cm^3 between sites with a median value of 0.052 cm^3/cm^3. After removing the bias, the SMAP product had a median ubRMSE of 0.036 cm^3/cm^3 (range from 0.024 to 0.083 cm^3/cm^3). Therefore, the SMAP product achieved the accuracy requirement of 0.04 cm^3/cm^3 (Chan et al., 2016) in this study area. The R value ranged from 0.075 to 0.81 with a median value of 0.59. The relationship between SMAP-derived and in-situ observed surface SM was significant ($p<0.05$) at all but one station. This suggests that the SMAP surface product can represent the temporal dynamics of the observed surface SM time series.

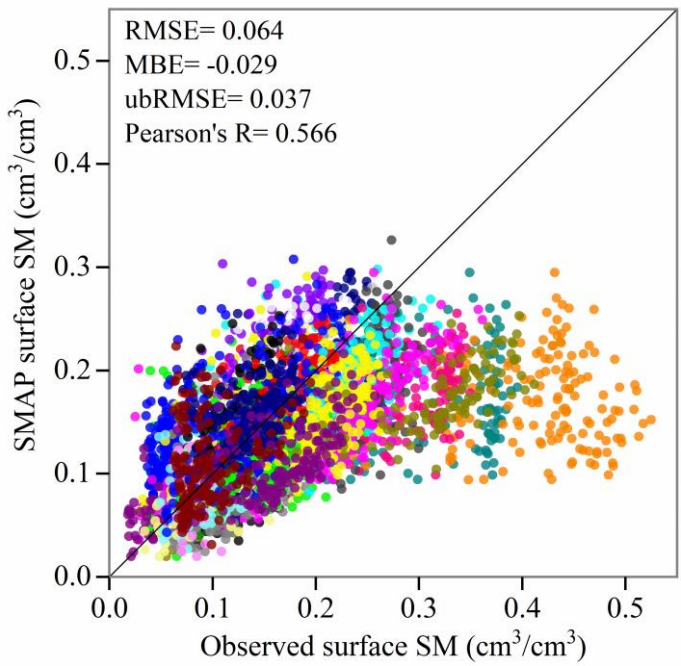

Fig. 6. Scatterplot of the SMAP_L3 surface SM (cm^3/cm^3) with in-situ observations at the surface (5 cm) of the 35 soil moisture stations. Each color indicated one station. Averaged metrics (RMSE, MBE, R, ubRMSE) of 35 stations during the growing seasons of 2015 and 2016 were showed in the plot.

4.3.2 SMAP-based estimation of subsurface soil moisture

For the estimation of subsurface soil moisture from the SMAP_L3 surface product, the site-specific T_{opt} was calculated based on the best match between SMAP estimations and in-situ observations in terms of NSE. The median values of T_{opt} for the layers 2, 3, 4, 5 and profile are 7 days, 12 days, 22 days, 35 days and 10 days, respectively. The subsurface SWI estimated from the combination of SMAP surface soil moisture with the ExpF method (with the median values of T_{opt}) were compared with the in-situ observations. A comparison of the subsurface SWI time series for different layers at each station are provided in Fig. S3- S7. Fig.7 shows the scatter plot between measured and predicted SWI, and the performance metrics are summarized in Table 4.

Table 4. Performance metrics (RSR, R, NSE) for the comparison of SMAP estimated and observed SWI at different layers for the 35 stations during the growing seasons of 2015-2016.

Layer	RSR		R		NSE	
	Mean±Std	Median	Mean±Std	Median	Mean±Std	Median
Layer 2 a	1.24±1.31	0.92	0.58±0.28	0.69	0.06±0.37	0.18
Layer 3 ab	1.28±0.83	1.11	0.45±0.35	0.55	-0.08±0.41	-0.02
Layer 4 b	1.49±1.21	1.12	0.28±0.46	0.31	-0.18±0.37	-0.13
Layer 5 b	1.96±3.43	1.17	0.24±0.5	0.34	-0.15±0.39	-0.15
Profile a	1.22±0.82	0.92	0.55±0.3	0.65	0.08±0.41	0.14

Note: the different letters after the layers indicate that the difference is significant at $p<0.05$ (Kruskal-Wallis ANOVA)

As expected, the estimation accuracy of subsurface SM decreased with depth. The ANOVA results showed that the subsurface SM estimation accuracy for layer 2 (median value of RSR=0.92, R=0.69, NSE=0.18) and profile SM (RSR=0.92, R=0.65, NSE=0.14) were significantly higher than for layer 4 (RSR=1.12, R=0.31, NSE=-0.13) and layer 5 (RSR=1.17, R=0.34, NSE=-0.15) ($p<0.05$). The NSE values were positive for layer 2 and profile SM, while the NSE values for the other layers were negative. The negative MBE showed that subsurface SM was underestimated. The relationship between SMAP-derived and in-situ observed subsurface SM for layer 2 and profile SM was significant ($p<0.01$) at all but one station (D15). Thus, the SMAP surface product and ExpF method can be used to estimate the subsurface SM in the study area, especially for layer 2 (10-20 cm) and profile (0-70 cm) SM.

As suggested by Ford et al. (2014), we partitioned the error in the SMAP-based estimation of profile SWI ("SMAP-observed profile SWI", Fig. S8c) in errors associated with the ExpF method and errors due to SMAP observation differences to gain some insight into the error sources of SMAP-based estimates of profile SWI. For this, profile SWI estimated using the ExpF method from observed surface SWI was compared with in-situ observed profile SWI ("estimated-observed profile SWI") to assess errors of the ExpF method (Fig. S8(a)). In addition, SMAP-based and in-situ observed surface SWI ("SMAP-observed surface SWI") were compared to assess inherent errors of the SMAP product (Fig. S8 (b)). RMSE, R and MAE were used as the metrics to assess accuracy. The results of this analysis are summarized in Table 5.

Table 5. Statistics of the metrics (RSR, R, NSE) of the comparisons of estimated-observed profile SWI datasets, SMAP_L3-observed surface SWI datasets, SMAP_L3-observed profile SWI datasets, and SMAP_L4-observed profile SWI datasets for the 35 stations during the growing seasons of 2015-2016.

Comparisons	RSR		R		NSE	
	Mean±std	Median	Mean±std	Median	Mean±std	Median
Estimated-observed PSWI	0.86±1.00	0.68	0.88±0.11	0.9	0.56±0.32	0.64
SMAP_L3-observed SSWI	1.13±0.49	1.01	0.57±0.17	0.59	-0.09±0.52	-0.07
SMAP_L3-observed PSWI	1.22±0.82	0.92	0.55±0.3	0.65	0.08±0.41	0.14
SMAP_L4-observed PSWI	1.42±0.76	1.25	0.47±0.31	0.55	-0.49±0.68	-0.3

Note: e.g. Estimated-observed PSWI means the comparison of the estimated profile SWI and observed profile SWI.

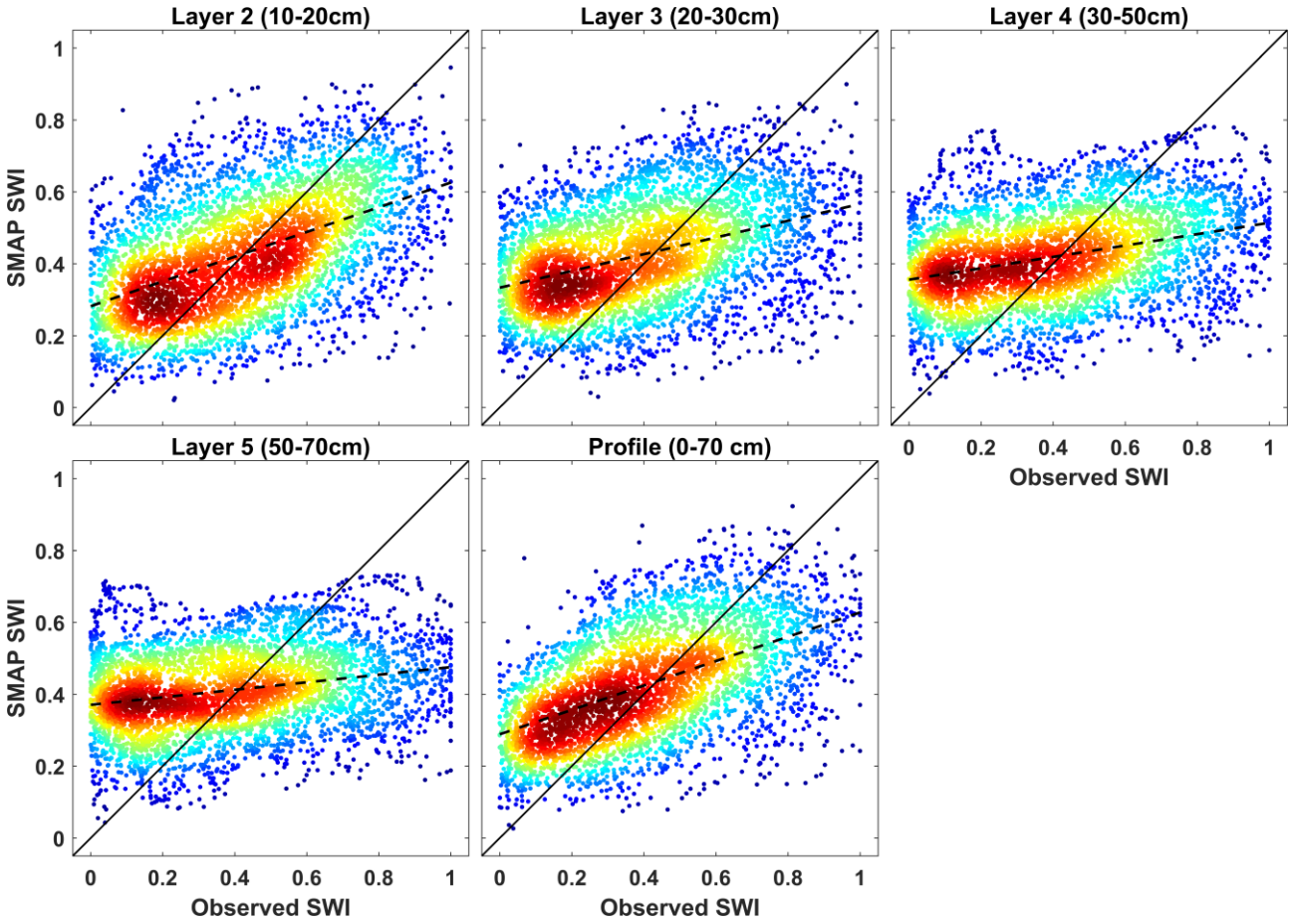

Fig. 7. Scatterplot of the comparisons of SMAP_L3 estimated-observed subsurface SWI for all stations during the growing seasons of 2015-2016. The representation is a smoothed color density of a scatter plot to make a quantity of points visual. The dash and solid line are the best-fitted curve and "y=x" line, respectively.

Fig. S8 and Table 5 show that the SMAP-observed SWI had lower performance metrics for surface SWI (median value of RSR, R and NSE are 1.01, 0.59 and -0.07, respectively) than for profile SWI (median value of RSR, R and NSE are 0.88, 0.72 and 0.19, respectively), which was similar to the results obtained from the Nebraska SM network (Ford et al., 2014). This may be because the profile SWI was estimated based on the SMAP surface SWI and T_{opt}, which was determined by optimization using the maximum NSE. This may have improved the performance of profile SWI estimation. In addition, the performance metrics for SMAP–observed SWI comparisons for both surface and profile SWI were significantly ($p<0.001$) lower than those of estimated–observed profile SWI (median value of RSR, R and NSE are 0.68, 0.90 and 0.64, respectively). Thus, the major error in SMAP-based profile SWI estimates stems from the SMAP satellite product and is not derived from the ExpF method, which is also supported by previous studies (e.g. Ford et al., 2014; Pablos et al., 2018). As mentioned before, the scale mismatch between point measurements and satellite footprints will introduce additional errors in the validation of the satellite-derived subsurface products (Jin et al. 2017).

Subsequently, the SMAP_L4 and SMAP_L3 estimated profile SWI were compared to the in situ observed profile SWI (see Fig. S10 and Table 5). From these results, we can see that the performance of profile soil moisture estimation using the SMAP_L3 surface product and the ExpF method (median RSR, R and NSE of 0.92, 0.65 and 0.14, respectively) was significantly ($p<0.01$) better than that of the SMAP_L4 product (median RSR, R and NSE of 1.25, 0.55 and -0.3, respectively). The low performance of the SMAP_L4 profile product may be associated with uncertainty in the meteorological driving forces and the soil parameters in the NASA catchment model for cold mountainous areas (Reichle et al., 2017; Zhao et al., 2018; Dai et al., 2019). Thus, our results suggest that combining the exponential filter method with the SMAP_L3 product improves the estimation of profile SM for the data-scarce cold arid mountainous areas significantly.

Finally, the spatial distribution of profile soil moisture during the growing season of 2015, 2016 and 2017 was obtained using the median value of T_{opt} and the SMAP_L3 product to get the spatial distribution of profile SM in the study area (Fig. 8). The spatial distribution of the profile SM shows higher values in the southeast, while lower values were obtained in the northwestern part of the study area. This distribution coincides with the spatial distribution of precipitation and surface SM. The temporal variation of profile SWI, surface SWI, and precipitation are shown in Fig. S10. Our results show that the temporal variation of the SM profile corresponded well with the occurrence of precipitation: Profile SM increased from May (mean SM of 0.27) to September (0.533) and then decreased until October (0.304). Profile SWI_{SMAP} was lower than surface SWI_{SMAP} from May to August, while profile SWI_{SMAP} was higher than surface SWI_{SMAP} from September to October. This can be attributed to the higher sensitivity of surface SM dynamics to precipitation and evapotranspiration (ET). During the months of September and October, less precipitation and higher ET caused a faster decrease in surface SM compared to profile SM.

Previous studies have shown the difficulty of applying the ExpF method to satellite products in mountainous area, where complex topography (Paulik et al., 2014), snow and soil freezing (Ford et al., 2014; Pablos et al., 2018) cause large errors and poor performance of the filtering method (Albergel et al., 2008). Ford et al. (2014) found an improvement of performance after removing the effects of snow from the data in the SCAN network, USA. Based on in situ SM observations, this study showed that the ExpF method is useful in estimating profile SM from SMAP surface products in the growing season in high and cold mountainous areas.

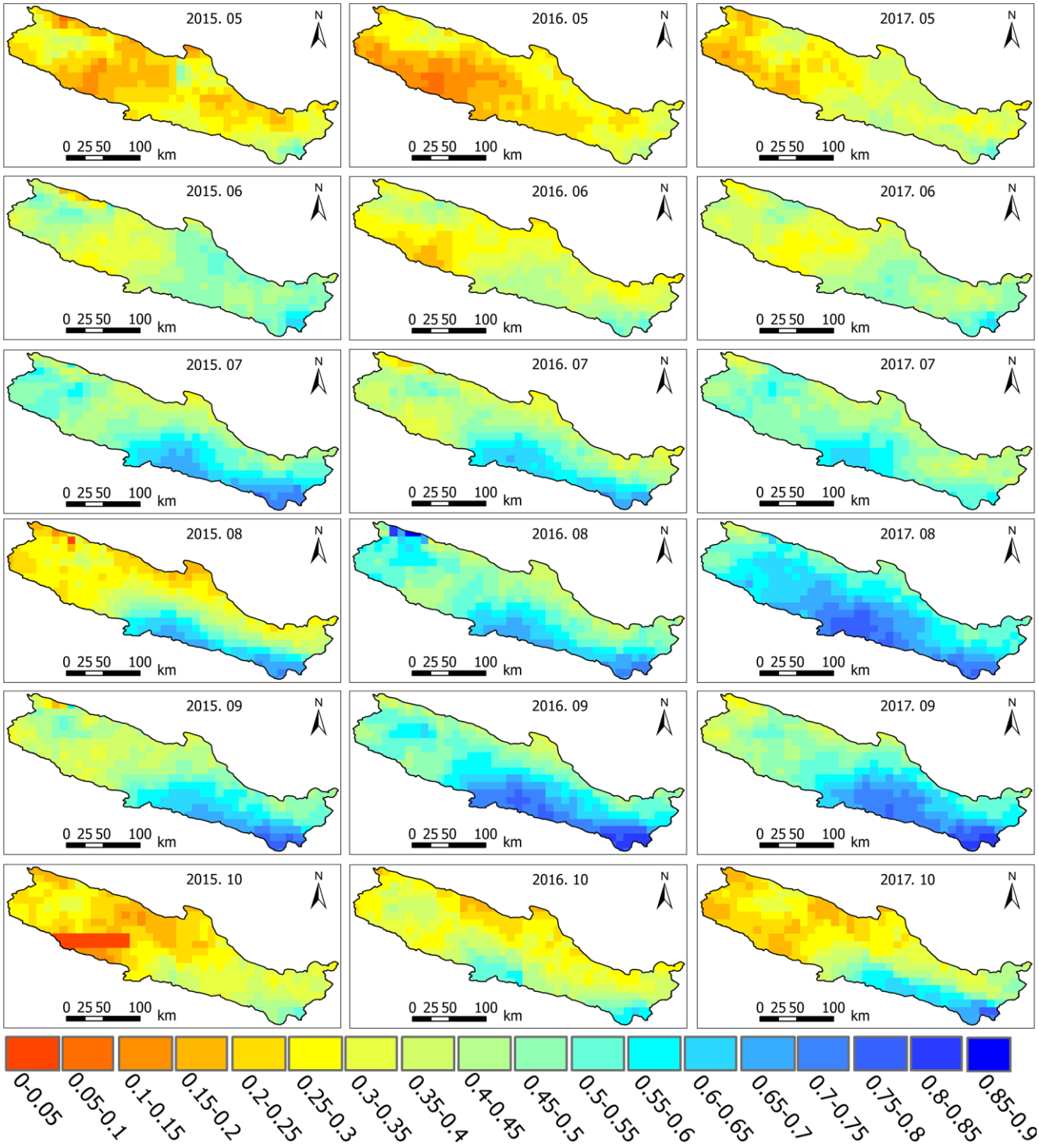

370 **Fig. 8.** The spatial distribution of the monthly averaged profile SWI product estimated from SMAP_L3 surface product during the growing season from 2015 to 2017. The title of each subplot provides the month and year.

5. Conclusions

In this study three methods (the exponential filter (ExpF), the artificial neural network (ANN) and the cumulative distribution function matching (CDF) methods) were used to calculate subsurface SM from in-situ surface SM observations at 5 cm depth in the Qilian Mountains (China). We also evaluated the utility of the ExpF method to estimate profile SM from SMAP surface products in the study area. Our main findings are:

1) With increasing depth of the predicted soil layer, the accuracy of all three methods decreased. Both the ANN and ExpF methods showed good performance for the estimation of SM down to 30 cm.

2) The ANN method exhibited the lowest estimation error, while the ExpF method was able to better capture the temporal variation of subsurface SM.

3) The area-generalized T_{opt} value of the ExpF method can be used in the study area to estimate the subsurface SM without significantly reducing the performance compared to a station-specific T_{opt}.

4) Subsurface SM derived from the SMAP_L3 surface SM product using the ExpF method showed less deviation from the in-situ observations compared to the SMAP_L4 root zone product for the study area.

We anticipate that our findings can improve the large-scale estimation of subsurface SM in mountainous areas, which in turn will support ecohydrological research and water resources management in inland river basins.

Data availability. All the data used in this research are available upon request.

Author contributions. BZ and CH prepared the research project. JT, ZH, CH, HB and JH conceptualized the methodology. JT, ZH and CM collected the data. JT, ZH and HB developed the code and performed the analysis. JT prepared the manuscript with contributions from all co-authors.

Competing interests. The authors declare that they have no conflict of interest

Acknowledgements:

The project is partially funded by the National Natural Science Foundation of China (grants 41530752, 51609111 and 91125010) and Fundamental Research Funds for the Central Universities (lzujbky-2016-256). We are grateful to the members of the Center for Dryland Water Resources Research and Watershed Science, Lanzhou University for their efforts to collect the soil moisture data and maintain the stations in this high, cold, and inaccessible mountainous area. Without their hard work, the soil moisture data presented in this paper would not have been available. We also thank the National Tibetan Plateau Data Centre (https://data.tpdc.ac.cn/en/) for providing supporting data. The first author also wishes to express his appreciation for the assistance and friendship that he experienced during his stay at the Forschungszentrum Jülich from September 2017 to March 2019.

References

Albergel, C., Rüdiger, C., Pellarin, T., Calvet, J.-C., Fritz, N., Froissard, F., Suquia, D., Petitpa, A., Piguet, B., and Martin, E.: From near-surface to root-zone soil moisture using an exponential filter: an assessment of the method based on in-situ observations and model simulations, Hydrol. Earth Syst. Sci., 12, 1323-1337, https://doi.org/10.5194/hess-12-1323-2008, 2008.

Bojinski, S., Verstraete, M., Peterson, T. C., Richter, C., Simmons, A., and Zemp, M.: The concept of essential climate variables in support of climate research, applications, and policy, Bull. Am. Meteorol. Soc., 95, 1431-1443, https://doi.org/10.1175/bams-d-13-00047.1, 2014.

Brocca, L., Melone, F., Moramarco, T., Wagner, W., Naeimi, V., Bartalis, Z., and Hasenauer, S.: Improving runoff prediction through the assimilation of the ASCAT soil moisture product, Hydrol. Earth Syst. Sci., 14, 1881-1893, https://doi.org/10.5194/hess-14-1881-2010, 2010.

Brocca, L., Hasenauer, S., Lacava, T., Melone, F., Moramarco, T., Wagner, W., Dorigo, W., Matgen, P., Martínez-Fernández, J., Llorens, P., Latron, J., Martin, C., and Bittelli, M.: Soil moisture estimation through ASCAT and AMSR-E sensors: An intercomparison and validation study across Europe, Remote Sens. Environ., 115, 3390-3408, https://doi.org/10.1016/j.rse.2011.08.003, 2011.

Brocca, L., Ciabatta, L., Massari, C., Camici, S., and Tarpanelli, A.: Soil Moisture for Hydrological Applications: Open Questions and New Opportunities, Water, 9, 140, https://doi.org/10.3390/w9020140, 2017.

Ceballos, A., Scipal, K., Wagner, W., and Martinez-Fernandez, J.: Validation of ERS scatterometer-derived soil moisture data in the central part of the Duero Basin, Spain, Hydrol. Process., 19, 1549-1566, https://doi.org/10.1002/hyp.5585, 2005.

Chan, S. K., Bindlish, R., O'Neill, P. E., Njoku, E., Jackson, T., Colliander, A., Chen, F., Burgin, M., Dunbar, S., and Piepmeier, J.: Assessment of the SMAP passive soil moisture product, IEEE Trans. Geosci. Remote Sens., 54, 4994-5007, https://doi.org/10.1109/TGRS.2016.2561938, 2016.

Chen, Y., Yang, K., He, J., Qin, J., Shi, J., Du, J., and He, Q.: Improving land surface temperature modeling for dry land of China, J. Geophys. Res.: Atmos., 116, https://doi.org/10.1029/2011jd015921, 2011.

Chen, Y., Yang, K., Qin, J., Cui, Q., Lu, H., La, Z., Han, M., and Tang, W.: Evaluation of SMAP, SMOS and AMSR2 soil moisture retrievals against observations from two networks on the Tibetan Plateau, J. Geophys. Res.: Atmos., https://doi.org/10.1002/2016JD026388, 2017.

Cihlar, J., Manak, D., and D'Iorio, M.: Evaluation of Compositing Algorithms for AVHRR Data over Land, IEEE T. Geosci. Remote., 32(2), 427-437. https://doi.org/10.1109/36.295057, 1994.

Cobos, D. R., and Chambers, C.: Calibrating ECH2O soil moisture sensors, Application Note, Decagon Devices, Pullman, WA, 2010.

Colliander, A., Jackson, T. J., Bindlish, R., Chan, S., Das, N., Kim, S., Cosh, M., Dunbar, R., Dang, L., and Pashaian, L.: Validation of SMAP surface soil moisture products with core validation sites, Remote Sens. Environ., 191, 215-231, https://doi.org/10.1016/j.rse.2017.01.021, 2017.

Dai, Y., Shangguan, W., Wei, N., Xin, Q., Yuan, H., Zhang, S., Liu, S., Lu, X., Wang, D., and Yan, F.: A review of the global soil property maps for Earth system models, SOIL, 5, 137-158, https://doi.org/10.5194/soil-5-137-2019, 2019.

De Lannoy, G. J. M., Houser, P. R., Verhoest, N. E. C., Pauwels, V. R. N., and Gish, T. J.: Upscaling of point soil moisture measurements to field averages at the OPE3 test site, J. Hydrol., 343, 1-11, https://doi.org/10.1016/j.jhydrol.2007.06.004, 2007.

Dobriyal, P., Qureshi, A., Badola, R., and Hussain, S. A.: A review of the methods available for estimating soil moisture and its implications for water resource management, J. Hydrol., 458, 110-117, https://doi.org/10.1016/j.jhydrol.2012.06.021, 2012.

Drusch, M., Wood, E. F., and Gao, H.: Observation operators for the direct assimilation of TRMM microwave imager retrieved soil moisture, Geophys. Res. Lett., 32, https://doi.org/10.1029/2005GL023623, 2005.

Entekhabi, D., Yueh, S., O'Neill, P. E., Kellogg, K. H., Allen, A., Bindlish, R., Brown, M., Chan, S., Colliander, A., and Crow, W. T.: SMAP handbook–soil moisture active passive: Mapping soil moisture and freeze/thaw from space, 2014.

Escorihuela, M.-J., Chanzy, A., Wigneron, J.-P., and Kerr, Y.: Effective soil moisture sampling depth of L-band radiometry: A case study, Remote Sens. Environ., 114, 995-1001, https://doi.org/10.1016/j.rse.2009.12.011, 2010.

Feng, Q., Yang, L., Deo, R. C., AghaKouchak, A., Adamowski, J. F., Stone, R., Yin, Z., Liu, W., Si, J., Wen, X., Zhu, M., and Cao, S.: Domino effect of climate change over two millennia in ancient China's Hexi Corridor, Nat. Sustainability, 2, 957-961, https://doi.org/10.1038/s41893-019-0397-9, 2019.

Ford, T. W., Harris, E., and Quiring, S. M.: Estimating root zone soil moisture using near-surface observations from SMOS, Hydrol. Earth Syst. Sci., 18, 139-154, https://doi.org/10.5194/hess-18-139-2014, 2014.

Gao, X., Li, H., Zhao, X., Ma, W., and Wu, P.: Identifying a suitable revegetation technique for soil restoration on water-limited and degraded land: Considering both deep soil moisture deficit and soil organic carbon sequestration, Geoderma, 319, 61-69, https://doi.org/10.1016/j.geoderma.2018.01.003, 2018.

Gao, X., Zhao, X., Brocca, L., Pan, D., and Wu, P.: Testing of observation operators designed to estimate profile soil moisture from surface measurements, Hydrol. Process., 33, 575-584, https://doi.org/10.1002/hyp.13344, 2019.

Georgakakos, K. P., Bae, D.-H., and Cayan, D. R.: Hydroclimatology of Continental Watersheds: 1. Temporal Analyses, Water Resour. Res., 31, 655-675, https://doi.org/10.1029/94WR02375, 1995.

González-Zamora, Á., Sánchez, N., Martínez-Fernández, J., and Wagner, W.: Root-zone plant available water estimation using the SMOS-derived soil water index, Adv. Water Resour., 96, 339-353, https://doi.org/10.1016/j.advwatres.2016.08.001, 2016.

Green, J. K., Seneviratne, S. I., Berg, A. M., Findell, K. L., Hagemann, S., Lawrence, D. M., and Gentine, P.: Large influence of soil moisture on long-term terrestrial carbon uptake, Nature, 565, 476-479, https://doi.org/10.1038/s41586-018-0848-x, 2019.

Han, E., Heathman, G. C., Merwade, V., and Cosh, M. H.: Application of observation operators for field scale soil moisture averages and variances in agricultural landscapes, J. Hydrol., 444-445, 34-50, https://doi.org/10.1016/j.jhydrol.2012.03.035, 2012.

Han, X., Hendricks Franssen, H.-J., Li, X., Zhang, Y., Montzka, C., and Vereecken, H.: Joint assimilation of surface temperature and L-band microwave brightness temperature in land data assimilation, Vadose Zone J., 12, https://doi.org/10.2136/vzj2012.0072, 2013.

He, C.S., Zhang, L.,H. and Wang, Y.: Impacts of Heterogeneity of Soil Hydraulic Properties on Watershed Hydrological Processes, Science Press, Beijing, 2018. (In Chinese with Engligh abstract)

Huete, A., Didan, K., Miura, T., Rodriguez, E.P., Gao, X., and Ferreira, L.G.: Overview of The Radiometric and Biophysical Performance of The MODIS Vegetation Indices. Remote Sens. Environ., 83, 10.1016/s0034-4257(02)00096-2, 2002.

Jakobi, J., Huisman, J., Vereecken, H., Diekkrüger, B., and Bogena, H.: Cosmic Ray Neutron Sensing for Simultaneous Soil Water Content and Biomass Quantification in Drought Conditions, Water Resour. Res., 54, 7383-7402, https://doi.org/10.1029/2018wr022692, 2018.

Jianxiu, Q., T., C. W., S., N. G., Xingguo, M., and Suxia, L.: The impact of vertical measurement depth on the information content of soil moisture times series data, Geophys. Res. Lett., 41, 4997-5004, https://doi.org/10.1002/2014gl060017, 2014.

Jin, R., Li, X., and Liu, S. M.: Understanding the Heterogeneity of Soil Moisture and Evapotranspiration Using Multiscale Observations From Satellites, Airborne Sensors, and a Ground-Based Observation Matrix, IEEE Geosci. Remote Sens. Lett., 14, 2132-2136, https://doi.org/10.1109/LGRS.2017.2754961, 2017.

Jin, X., Zhang, L. h., Gu, J., Zhao, C., Tian, J., and He, C. S.: Modeling the impacts of spatial heterogeneity in soil hydraulic properties on hydrological process in the upper reach of the Heihe River in the Qilian Mountains, Northwest China, Hydrol. Processes, 29, 3318-3327, 10.1002/hyp.10437, 2015.

Jonard, F., Bogena, H., Caterina, D., Garré, S., Klotzsche, A., Monerris, A., Schwank, M., and von Hebel, C.: Ground-Based Soil Moisture Determination, in: Observation and Measurement, edited by: Li, X., and Vereecken, H., Springer, Berlin, Heidelberg, 1-42, 2018.

Jung, M., Reichstein, M., Ciais, P., Seneviratne, S. I., Sheffield, J., Goulden, M. L., Bonan, G., Cescatti, A., Chen, J., de Jeu, R., Dolman, A. J., Eugster, W., Gerten, D., Gianelle, D., Gobron, N., Heinke, J., Kimball, J., Law, B. E., Montagnani, L., Mu, Q., Mueller, B., Oleson, K., Papale, D., Richardson, A. D., Roupsard, O., Running, S., Tomelleri, E., Viovy, N., Weber, U., Williams, C., Wood, E., Zaehle, S., and Zhang, K.: Recent decline in the global land evapotranspiration trend due to limited moisture supply, Nature, 467, 951, http://dx.doi.org/10.1038/nature09396, 2010.

Kornelsen, K. C., and Coulibaly, P.: Root-zone soil moisture estimation using data-driven methods, Water Resour. Res., 50, 2946-2962, https://doi.org/10.1002/2013WR014127, 2014.

Lange, R. d., Beck, R., Giesen, N. v. d., Friesen, J., Wit, A. d., and Wagner, W.: Scatterometer-Derived Soil Moisture Calibrated for Soil Texture With a One-Dimensional Water-Flow Model, IEEE Trans. Geosci. Remote Sens., 46, 4041-4049, https://doi.org/10.1109/TGRS.2008.2000796, 2008.

Li, X., Liu, S., Xiao, Q., Ma, M., Jin, R., Che, T., Wang, W., Hu, X., Xu, Z., and Wen, J.: A multiscale dataset for understanding complex eco-hydrological processes in a heterogeneous oasis system, Sci. Data, 4, 170083, https://doi.org/10.1038/sdata.2017.83, 2017.

Li, X., Cheng, G. D., Ge, Y. C., Li, H. Y., Han, F., Hu, X. L., Tian, W., Tian, Y., Pan, X. D., Nian, Y. Y., Zhang, Y. L., Ran, Y. H., Zheng, Y., Gao, B., Yang, D. W., Zheng, C. M., Wang, X. S., Liu, S. M., and Cai, X. M.: Hydrological Cycle in the Heihe River Basin and Its Implication for Water Resource Management in Endorheic Basins, J. Geophys. Res.: Atmos., 123, 890-914, https://doi.org/10.1002/2017jd027889, 2018.

Li, Z., Xu, Z., Shao, Q., and Yang, J.: Parameter estimation and uncertainty analysis of SWAT model in upper reaches of the Heihe river basin, Hydrol. Process., 23, 2744-2753, https://doi.org/10.1002/hyp.7371, 2009.

Liu, H., Zhao, W., He, Z., and Liu, J.: Soil moisture dynamics across landscape types in an arid inland river basin of Northwest China, Hydrol. Process., 29, 3328-3341, https://doi.org/10.1002/hyp.10444, 2015.

Liu, J., Chai, L., Lu, Z., Liu, S., Qu, Y., Geng, D., Song, Y., Guan, Y., Guo, Z., and Wang, J.: Evaluation of SMAP, SMOS-IC, FY3B, JAXA, and LPRM Soil Moisture Products over the Qinghai-Tibet Plateau and Its Surrounding Areas, Remote Sens., 11, 792, https://doi.org/10.3390/rs11070792, 2019.

Liu, S., Li, X., Xu, Z., Che, T., Xiao, Q., Ma, M., Liu, Q., Jin, R., Guo, J., Wang, L., Wang, W., Qi, Y., Li, H., Xu, T., Ran, Y., Hu, X., Shi, S., Zhu, Z., Tan, J., Zhang, Y., and Ren, Z.: The Heihe Integrated Observatory Network: A Basin-Scale Land Surface Processes Observatory in China, Vadose Zone J., 17, https://doi.org/10.2136/vzj2018.04.0072, 2018a.

Liu, Z., Cheng, L., Hao, Z., Li, J., Thorstensen, A., and Gao, H.: A framework for exploring joint effects of conditional factors on compound floods, Water Resour. Res., 54, 2681-2696, 2018b.

Luo, K., Tao, F., Moiwo, J. P., and Xiao, D.: Attribution of hydrological change in Heihe River Basin to climate and land use change in the past three decades, Sci. Rep., 6, 33704, https://doi.org/10.1038/srep33704, 2016.

Mahmood, R., and Hubbard, K. G.: Relationship between soil moisture of near surface and multiple depths of the root zone under heterogeneous land uses and varying hydroclimatic conditions, Hydrol. Process., 21, 3449-3462, https://doi.org/doi:10.1002/hyp.6578, 2007.

Manfreda, S., Brocca, L., Moramarco, T., Melone, F., and Sheffield, J.: A physically based approach for the estimation of root-zone soil moisture from surface measurements, Hydrol. Earth Syst. Sci., 18, 1199-1212, https://doi.org/10.5194/hess-18-1199-2014, 2014.

Moriasi, D. N., Arnold, J. G., Van Liew, M. W., Bingner, R. L., Harmel, R. D., and Veith, T. L.: Model evaluation guidelines for systematic quantification of accuracy in watershed simulations, Trans. ASABE, 50, 885-900, https://doi.org/10.13031/2013.23153, 2007.

Muhammad, Z., Hyunglok, K., and Minha, C.: Evaluating the patterns of spatiotemporal trends of root zone soil moisture in major climate regions in East Asia, J. Geophys. Res.: Atmos., 122, 7705-7722, https://doi.org/10.1002/2016JD026379, 2017.

Ochsner, T. E., Cosh, M. H., Cuenca, R. H., Dorigo, W. A., Draper, C. S., Hagimoto, Y., Kerr, Y. H., Larson, K. M., Njoku, E. G., Small, E. E., and Zreda, M.: State of the Art in Large-Scale Soil Moisture Monitoring, Soil Sci. Soc. Am. J., 77, 1888-1919, https://doi.org/10.2136/sssaj2013.03.0093, 2013.

Pablos, M., González-Zamora, Á., Sánchez, N., and Martínez-Fernández, J.: Assessment of Root Zone Soil Moisture Estimations from SMAP, SMOS and MODIS Observations, Remote Sens., 10, 981, https://doi.org/10.3390/rs10070981, 2018.

Pan, Q. M., and Tian, S. L.: Water resources in the Heihe river basin, The Yellow River Water Conservency Press, Zheng Zhou, China, 2001. (In Chinese)

Pan, X., Kornelsen, K. C., and Coulibaly, P.: Estimating Root Zone Soil Moisture at Continental Scale Using Neural Networks, J. Am. Water Resour. Assoc., 53, 220-237, https://doi.org/10.1111/1752-1688.12491, 2017.

Pasolli, L., Notarnicola, C., Bruzzone, L., Bertoldi, G., Della Chiesa, S., Hell, V., Niedrist, G., Tappeiner, U., Zebisch, M., and Del Frate, F.: Estimation of soil moisture in an alpine catchment with RADARSAT2 images, Appl. Environ. Soil Sci., 2011, http://dx.doi.org/10.1155/2011/175473, 2011.

Paulik, C., Dorigo, W., Wagner, W., and Kidd, R.: Validation of the ASCAT Soil Water Index using in situ data from the International Soil Moisture Network, Int. J. Appl. Earth Obs. Geoinf., 30, 1-8, https://doi.org/10.1016/j.jag.2014.01.007, 2014.

Peng, J., Loew, A., Merlin, O., and Verhoest, N. E.: A review of spatial downscaling of satellite remotely sensed soil moisture, Rev. Geophys., 55, https://doi.org/10.1002/2016RG000543, 2017.

Qiu, J., Crow, W. T., Nearing, G. S., Mo, X., and Liu, S.: The impact of vertical measurement depth on the information content of soil moisture times series data, Geophys. Res. Lett., 41, 4997-5004, https://doi.org/10.1002/2014GL060017, 2014.

Qu, Y., Zhu, Z., Chai, L., Liu, S., Montzka, C., Liu, J., Yang, X., Lu, Z., Jin, R., and Li, X.: Rebuilding a Microwave Soil Moisture Product Using Random Forest Adopting AMSR-E/AMSR2 Brightness Temperature and SMAP over the Qinghai–Tibet Plateau, China, Remote Sens., 11, 683, https://doi.org/10.3390/rs11060683, 2019.

Rasmy, M., Koike, T., Boussetta, S., Lu, H., and Li, X.: Development of a satellite land data assimilation system coupled with a mesoscale model in the Tibetan Plateau, IEEE Trans. Geosci. Remote Sens., 49, 2847-2862, https://doi.org/10.1109/TGRS.2011.2112667, 2011.

Reichle, R. H., and Koster, R. D.: Bias reduction in short records of satellite soil moisture, Geophys. Res. Lett., 31, https://doi.org/10.1029/2004GL020938, 2004.

Reichle, R. H., Lannoy, G. J. M. D., Liu, Q., Ardizzone, J. V., Colliander, A., Conaty, A., Crow, W., Jackson, T. J., Jones, L. A., Kimball, J. S., Koster, R. D., Mahanama, S. P., Smith, E. B., Berg, A., Bircher, S., Bosch, D., Caldwell, T. G., Cosh, M., González-Zamora, Á., Collins, C. D. H., Jensen, K. H., Livingston, S., Lopez-Baeza, E., Martínez-Fernández, J., McNairn, H., Moghaddam, M., Pacheco, A., Pellarin, T., Prueger, J., Rowlandson, T., Seyfried, M., Starks, P., Su, Z., Thibeault, M.,

Velde, R. v. d., Walker, J., Wu, X., and Zeng, Y.: Assessment of the SMAP Level-4 Surface and Root-Zone Soil Moisture Product Using In Situ Measurements, J. Hydrometeorol., 18, 2621-2645, https://doi.org/10.1175/jhm-d-17-0063.1, 2017.

Seneviratne, S. I., Corti, T., Davin, E. L., Hirschi, M., Jaeger, E. B., Lehner, I., Orlowsky, B., and Teuling, A. J.: Investigating soil moisture–climate interactions in a changing climate: a review, Earth Sci. Rev., 99, 125-161, https://doi.org/10.1016/j.earscirev.2010.02.004, 2010.

Tian, J., Zhang, B., He, C., and Yang, L.: Variability in Soil Hydraulic Conductivity and Soil Hydrological Response Under Different Land Covers in the Mountainous Area of the Heihe River Watershed, Northwest China, Land Degrad. Dev., 28, 1437-1449, https://doi.org/10.1002/ldr.2665, 2017.

Tian, J., Zhang, B., He, C., Han, Z., Bogena, H. R., and Huisman, J. A.: Dynamic response patterns of profile soil moisture wetting events under different land covers in the Mountainous area of the Heihe River Watershed, Northwest China, Agric. For. Meteorol., 271, 225-239, https://doi.org/10.1016/j.agrformet.2019.03.006, 2019.

Tobin, K. J., Torres, R., Crow, W. T., and Bennett, M. E.: Multi-decadal analysis of root-zone soil moisture applying the exponential filter across CONUS, Hydrol. Earth Syst. Sci., 21, 4403-4417, https://doi.org/10.5194/hess-21-4403-2017, 2017.

Ullah, W., Wang, G., Gao, Z., Hagan, D. F. T., and Lou, D.: Comparisons of remote sensing and reanalysis soil moisture products over the Tibetan Plateau, China, Cold Reg. Sci. Technol., 146, 110-121, https://doi.org/10.1016/j.coldregions.2017.12.003, 2018.

Wagner, W., Lemoine, G., and Rott, H.: A method for estimating soil moisture from ERS scatterometer and soil data, Remote Sens. Environ., 70, 191-207, https://doi.org/10.1016/s0034-4257(99)00036-x, 1999.

Wang, S., Fu, B., Gao, G., Zhou, J., Jiao, L., and Liu, J.: Linking the soil moisture distribution pattern to dynamic processes along slope transects in the Loess Plateau, China, Environ. Monit. Assess., 187, 778, https://doi.org/10.1007/s10661-015-5000-x, 2015.

Wang, T., Franz, T. E., You, J., Shulski, M. D., and Ray, C.: Evaluating controls of soil properties and climatic conditions on the use of an exponential filter for converting near surface to root zone soil moisture contents, J. Hydrol., 548, 683-696, https://doi.org/10.1016/j.jhydrol.2017.03.055, 2017.

Williams, C., McNamara, J., and Chandler, D.: Controls on the temporal and spatial variability of soil moisture in a mountainous landscape: the signature of snow and complex terrain, Hydrol. Earth Syst. Sci., 13, 1325-1336, https://doi.org/10.5194/hess-13-1325-2009, 2009.

Wu Jinhua, Zhong Bo, and Wu Junjun.: Landsat-based continuous monthly 30m×30m land surface NDVI dataset in Qilian Mountain area (1986-2017). National Tibetan Plateau Data Center, doi: 10.11888/Geogra.tpdc.270136, 2019.

Wu, W., Geller, M. A., and Dickinson, R. E.: The response of soil moisture to long-term variability of precipitation, J. Hydrometeorol., 3, 604-613, https://doi.org/10.1175/1525-7541(2002)003<0604:TROSMT>2.0.CO;2, 2002.

Xiaojun, P., C., K. K., and Paulin, C.: Estimating Root Zone Soil Moisture at Continental Scale Using Neural Networks, J. Am. Water Resour. Assoc., 53, 220-237, https://doi.org/doi:10.1111/1752-1688.12491, 2017.

Yao, Y., Zheng, C., Andrews, C., Zheng, Y., Zhang, A., and Liu, J.: What Controls the Partitioning between Baseflow and Mountain Block Recharge in the Qinghai-Tibet Plateau?, Geophys. Res. Lett., 44, 8352-8358, https://doi.org/10.1002/2017GL074344, 2017.

Zeng, J., Li, Z., Chen, Q., Bi, H., Qiu, J., and Zou, P.: Evaluation of remotely sensed and reanalysis soil moisture products over the Tibetan Plateau using in-situ observations, Remote Sens. Environ., 163, 91-110, https://doi.org/10.1016/j.rse.2015.03.008, 2015.

Zhang, L., He, C., and Zhang, M.: Multi-Scale Evaluation of the SMAP Product Using Sparse In-Situ Network over a High Mountainous Watershed, Northwest China, Remote Sens., 9, 1111, https://doi.org/10.3390/rs9111111, 2017b.

Zhang, N., Quiring, S., Ochsner, T., and Ford, T.: Comparison of Three Methods for Vertical Extrapolation of Soil Moisture in Oklahoma, Vadose Zone J., 16, https://doi.org/10.2136/vzj2017.04.0085, 2017a.

Zhao, H., Zeng, Y., Lv, S., and Su, Z.: Analysis of soil hydraulic and thermal properties for land surface modeling over the Tibetan Plateau, Earth Syst. Sci. Data, 10, 1031-1061, https://doi.org/10.5194/essd-10-1031-2018, 2018.

Zhao, L., Yang, K., Qin, J., Chen, Y., Tang, W., Montzka, C., Wu, H., Lin, C., Han, M., and Vereecken, H.: Spatiotemporal analysis of soil moisture observations within a Tibetan mesoscale area and its implication to regional soil moisture measurements, J. Hydrol., 482, 92-104, https://doi.org/10.1016/j.jhydrol.2012.12.033, 2013.

Zhao, L., Yang, K., Qin, J., Chen, Y., Tang, W., Lu, H., and Yang, Z.-L.: The scale-dependence of SMOS soil moisture accuracy and its improvement through land data assimilation in the central Tibetan Plateau, Remote Sens. Environ., 152, 345-355, https://doi.org/10.1016/j.rse.2014.07.005, 2014.

Zhao, W., and Li, A.: A comparison study on empirical microwave soil moisture downscaling methods based on the integration of microwave-optical/IR data on the Tibetan Plateau, Int. J. Remote Sens., 36, 4986-5002, https://doi.org/10.1080/01431161.2015.1041178, 2015.

Zhou, J., Cai, W., Qin, Y., Lai, L., Guan, T., Zhang, X., Jiang, L., Du, H., Yang, D., Cong, Z., and Zheng, Y.: Alpine vegetation phenology dynamic over 16years and its covariation with climate in a semi-arid region of China, Sci. Total Environ., 572, 119-128, https://doi.org/10.1016/j.scitotenv.2016.07.206, 2016.